# Exotic Vortex States with Discrete Rotational Symmetry in Atomic Fermi Gases with Spin-Orbital–Angular-Momentum Coupling

Liang-Liang Wang,[1,2] An-Chun Ji,[3] Qing Sun,[3,*] and Jian Li[1,2,†]
[1]School of Science, Westlake University, 18 Shilongshan Road, Hangzhou 310024, Zhejiang Province, China
[2]Institute of Natural Sciences, Westlake Institute for Advanced Study, 18 Shilongshan Road, Hangzhou 310024, Zhejiang Province, China
[3]Department of Physics, Key Lab of Terahertz Optoelectronics (MoE), Capital Normal University, Beijing 100048, China

(Received 10 July 2020; accepted 8 April 2021; published 12 May 2021)

We investigate the superfluidity of a two-component Fermi gas with spin-orbital-angular-momentum coupling (SOAMC). Because of the intricate interplay of SOAMC, two-photon detuning and atom-atom interaction, a family of vortex ground states emerges in a broad parameter regime of the phase diagram, in contrast to the usual case where an external rotation or magnetic field is generally required. More strikingly, an unprecedented vortex state, which breaks the continuous rotational symmetry to a discrete one spontaneously, is predicted to occur. The underlying physics are elucidated and verified by numerical simulations. The unique density distributions of the predicted vortex states enable a direct observation in experiment.

DOI: 10.1103/PhysRevLett.126.193401

*Introduction.*—In recent years, the realization of spin-orbit coupling (SOC) in ultracold atoms [1–6] has stimulated intensive studies on the searching of exotic quantum phases brought by SOC. For example, it can lead to unconventional Fermi superfluids [7–15], a supersolid stripe phase [16–18], and diverse magnetic phases [19–22]. Nevertheless, most of these studies have been focused on the coupling between spin and linear momentum [23–29]. More recently by coupling the atomic internal "spin" state to its orbital angular momentum, a new type of SOC, named spin-orbital-angular-momentum coupling (SOAMC), was proposed [30–32] and first realized in spinor BEC [33–35].

In the SOAMC scheme, a pair of copropagating high-order Laguerre-Gauassian (LG) lasers [36–39] with different orbital angular momenta is generally used to generate an effective coupling between the $z$ component of spin $\vec{\sigma}$ (Pauli representation) and orbital momentum $\vec{L} \equiv \vec{r} \times \vec{p}$ ($\vec{r}$, $\vec{p}$ denotes the position and momentum) in the form of

$$H_{\mathrm{SOAMC}} \sim \sigma_z \cdot L_z.$$

Compared to the SOC with linear momentum, the SOAMC breaks the translational symmetry while it keeps a typical rotational symmetry. This can significantly affect the many-body behaviors of the underlying systems and give rise to diverse topological excitations, e.g., the intriguing vortex states in BEC [33–35,40,41], which are hardly produced by SOC with linear momentum itself. Therefore, the SOAMC provides new features and advantages to explore the unusual superfluid states of a Fermi gas with rotational symmetry, which, however, has never been addressed so far.

In this Letter, we investigate the ground state of a two-dimensional (two-component) attractive Fermi gas with SOAMC. By numerically solving the Bogoliubov–de Gennes (BdG) equations self-consistently, we obtain the ground-state phase diagram of the system, which encapsulates rich physics. We show that a family of single-vortex ground states exists in a broad regime of the phase diagram for finite two-photon detuning, in contrast to the conventional case where an external rotation or magnetic field is required. Remarkably, an unprecedented vortex state, which spontaneously breaks the continuous rotational symmetry to a discrete one, is predicted to appear. Such state exhibits a periodical spatial modulation in the angular space, and can be detected in experiment. The underlying mechanism of these vortex states is elucidated to be the unconventional pairing with quantized orbital angular momentum between fermions, which originates from the interplay of SOAMC, two-photon detuning and atom-atom interaction. Such vortex states have no counterpart in the literatures and offer a unique opportunity to explore the exotic low-energy modes and macroscopic quantum phenomena in this system.

*The model.*—We consider a two-component Fermi gas confined in a two-dimensional geometry. As depicted in Fig. 1, the atoms are shined by two copropagating LG laser beams with opposite angular momenta $\pm l\hbar$ to induce an effective SOAMC along the $z$ axis via a two-photon Raman process between the two pseudospin states (labeled as $\uparrow$ and $\downarrow$). In the transformed basis, the single-particle Hamiltonian of the system can be written as (by setting $\hbar = M = 1$) [42]

 

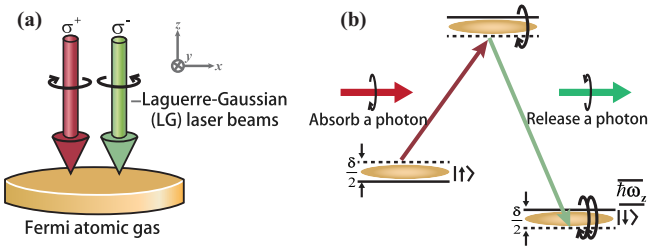


FIG. 1. Schematic of the setup (a) and energy levels (b). A pair of LG Raman laser beams with opposite orbital angular momenta $\pm\ell\hbar$ copropagates and generates SOAMC along the $z$ axis in the two-dimensional Fermi gas. $\delta$ is the two-photon detuning.

$$H_0 = -\frac{1}{2r}\frac{\partial^2}{\partial r^2}r + \frac{L_z^2+\ell^2}{2r^2} + \alpha(r)L_z\sigma_z + V_{\rm ho}(r) + \mathcal{L}(r),$$
$$\mathcal{L}(r) = \frac{\delta}{2}\sigma_z - \chi I(r) + \Omega I(r)\sigma_x, \quad (1)$$

where $L_z = -i\partial_\phi$ is the $z$ component of the angular momentum operator, which couples to the pseudospin $\sigma_z$ with inhomogeneous SOAMC strength $\alpha(r) = \ell/r^2$. $\delta$ is the two-photon detuning, the diagonal parameter $\chi$ is the ac Stark light shift and the off-diagonal term $\Omega$ is the effective two-photon Rabi frequency between two pseudospin states. The spatial intensity profile of the LG laser beams is given by $I(r) = [\sqrt{2}(r/w)]^{2|\ell|}[L_k^{|\ell|}(2r^2/w^2)e^{-r^2/w^2}]^2$, where $w$ characterizes the beam width, and $L_k^{|\ell|}$ is the generalized Laguerre polynomials with azimuthal index $\ell$ and the radial index $k$ describing the radial intensity distribution of the LG beams [32]. $V_{\rm ho}(r) = \omega_r^2 r^2/2$ is a harmonic trapping potential with frequency $\omega_r$. Without loss of generality, we consider the case with $\ell = 4$, $k = 0$, and $w = 2a_{\rm osc}$ with $a_{\rm osc} = \sqrt{1/\omega_r}$ being the harmonic oscillator length.

The single-particle Hamiltonian $H_0$ possesses a rotational symmetry with $[L_z, H_0] = 0$, such that the eigenstates can be labeled by two quantum numbers $(n, m)$ with energies $E_{n,m}$, where $n$ and $m$ are the radial and angular quantum number, respectively, giving rise to a discrete single-particle spectrum [42]. For $\delta = 0$, an additional time-reversal (TR) symmetry is held, i.e., $[T, H_0] = 0$, where $T = i\sigma_y K$ with $K$ the complex-conjugation operator. This rules out a single vortex ground state and one generally needs a magnetic field or an external rotation to break this symmetry to favor vortex states in a Fermi superfluid. While for $\delta \neq 0$, such TR symmetry is absent and we have $E_{n,m} \neq E_{n,-m}$. As shown below, this would significantly change the pairing between fermions, and a family of exotic vortex states with unusual properties emerges in the ground-state phase diagram.

*Ground-state phase diagram.*—To reveal the superfluid physics of the system, we consider the $s$-wave contact interaction $H_{\rm int} = g\int d\mathbf{r}\Psi_\uparrow^\dagger(\mathbf{r})\Psi_\downarrow^\dagger(\mathbf{r})\Psi_\downarrow(\mathbf{r})\Psi_\uparrow(\mathbf{r})$ with a bare interaction parameter $g < 0$, which is related to the two-body binding energy $E_b$ in two dimensions via $g = -4\pi/[\ln(1 + 2E_c/E_b)]$ [44], with $E_c$ being the energy cutoff. $\Psi_\sigma^\dagger(\mathbf{r})$ $[\Psi_\sigma(\mathbf{r})]$ creates (annihilates) a Fermi atom at position $\mathbf{r} \equiv (r, \phi)$ of spin $\sigma = \uparrow, \downarrow$. Introducing the superfluid order parameter $\Delta(\mathbf{r}) = g\langle\Psi_\downarrow(\mathbf{r})\Psi_\uparrow(\mathbf{r})\rangle$ and applying a Bogoliubov-Valation transformation, the resultant Bogoliubov–de Gennes equation is given by [42]

$$\begin{bmatrix} H_0 - \mu & \Delta(\mathbf{r}) \\ \Delta^*(\mathbf{r}) & -\sigma_y(H_0^* - \mu)\sigma_y \end{bmatrix}\Phi_\eta(\mathbf{r}) = E_\eta\Phi_\eta(\mathbf{r}), \quad (2)$$

with the Nambu representation $\Phi_\eta(\mathbf{r}) = [u_{\uparrow,\eta}(\mathbf{r}), u_{\downarrow,\eta}(\mathbf{r}), v_{\downarrow,\eta}(\mathbf{r}), -v_{\uparrow,\eta}(\mathbf{r})]^T$. $\mu$ is the chemical potential and $E_\eta$ is the energy of Bogoliubov quasiparticles labeled by an index $\eta$. In this basis, the order parameter $\Delta(\mathbf{r})$ can be written as

$$\Delta(\mathbf{r}) = g\sum_\eta [u_{\uparrow,\eta}(\mathbf{r})v_{\downarrow,\eta}^*(\mathbf{r})f(-E_\eta) - u_{\downarrow,\eta}(\mathbf{r})v_{\uparrow,\eta}^*(\mathbf{r})f(E_\eta)], \quad (3)$$

where $f(E) = 1/[e^{E/k_BT} + 1]$ is the Fermi-Dirac distribution at a temperature $T$, and the summation is over the quasiparticle state with $E_\eta \geq 0$. Self-consistently solving Eq. (4) and the number equation $N_{\rm atom} = \sum_\sigma \int d\mathbf{r} n_\sigma(\mathbf{r})$ with atomic density $n_\sigma(r) = \sum_\eta[|u_{\sigma,\eta}(r)|^2 f(E_\eta) + |v_{\sigma,\eta}(r)|^2 f(-E_\eta)]$, we can obtain the ground state of the system.

In Fig. 2(a), we present the ground-state phase diagram in the $\delta$-$E_b$ plane for fixed two-photon Rabi frequency $\Omega/E_F = 0.2$ and $\chi/E_F = 0.7$. There are three classes of phases: a normal superfluid (NS) with a real $\Delta \neq 0$ (up to a global phase), a normal gas (NG) with $\Delta = 0$ and single vortex states. Such a vortex is characterized by a complex $\Delta \neq 0$ with a nontrivial phase configuration, i.e., a $2\pi Q$ phase gradient with integer vorticity (winding number) $Q \neq 0$ along a closed path around the vortex [middle column in Fig. 2(b)]. For small $\delta$, the NS is dominant. While for sufficiently large $\delta$, the large energy mismatch between two spin states strongly suppresses the pairing and destroys the superfluid, resulting in a NG phase. In between, a family of vortex states with different vorticity $Q$ exist. In Fig. 2(a), we find the regimes for vortex with $Q = 1$ and $Q = 2$ (labeled as vortex-1 and vortex-2), and vortex states with higher $Q$ can be obtained for a larger $\delta$ and $E_b$ (not shown). As $Q$ is quantized, the transition between these phases are of first order.

Considering that an external rotation or magnetic field is generally desired to produce a vortex in a Fermi superfluid without SOAMC, it is quite interesting to see here that the quantum vortex may emerge as a ground state in the presence of SOAMC, suggesting a new mechanism responsible for the forming of vortex in this system. To gain insight, we can write the order parameter as

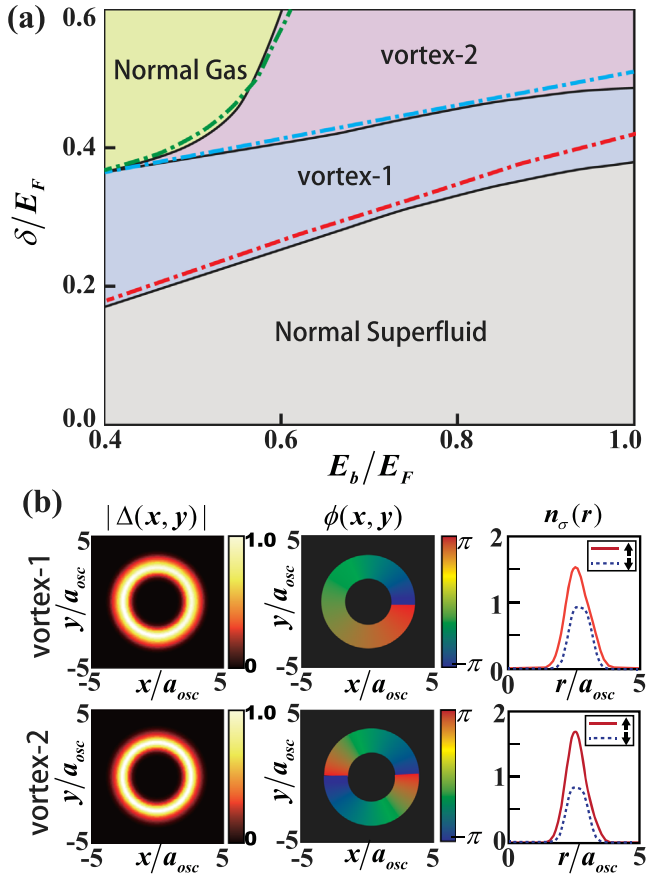


FIG. 2. (a) The ground-state phase diagram of the BdG simulations (solid lines) and the effective model (dash-dotted lines) in the $E_b$-$\delta$ plane for a superfluid Fermi gas with SOAMC. Vortex-$Q$ ($Q = 1, 2$) denotes a single-vortex state with velocity $Q$. (b) The spatial amplitude $|\Delta(x, y)|$ (left column) and phase $\phi(x, y)$ (middle column) of the order parameter for the vortex phases in (a), and the right column gives the corresponding atomic radial density $n_\sigma(r)$ for each vortex. Here we have taken $N_{\text{atom}} = 50$, $\chi/E_F = 0.7$ and $\Omega/E_F = 0.21$.

$\Delta = |\Delta(r)|e^{iQ\phi}$ for a single vortex with vorticity $Q$. This implies that pairing with finite orbital angular momentum, if possible, may play a key role in this system. As we will see, such exotic pairing state appears naturally from the interplay between SOAMC, two-photon detuning, and atom-atom interaction.

To grasp the main physics, we notice that the real space density distribution of the superfluid states has a sharp peak around $R = \sqrt{\ell/2w}$ along the radical direction [right column of Fig. 2(b)] due to the confinement of the red-detuned ac stark potential, it is reasonable to ignore the radial dependence by approximating $r \simeq R$, which leaves an effective one-dimensional model on a ring with the single-particle part $H_0^{\text{ring}} = -\partial_\phi^2/2R^2 - i\tilde{\alpha}\partial_\phi\sigma_z + (\delta/2)\sigma_z + \tilde{\Omega}\sigma_x$, where $\tilde{\alpha} = \ell/R^2$, $\tilde{\Omega} = \Omega I(R)$ are the effective SOAMC and Raman coupling, respectively. This Hamiltonian can be diagonalized straightforwardly in the basis $\{e^{im\phi}\}$ with $m$ the quantum number of orbital angular momentum. The resultant single-particle energy spectrum has two branches $E_\pm(m) = m^2/2R^2 \pm \sqrt{\tilde{\Omega}^2 + (\tilde{\alpha}m + \delta/2)^2}$. The above results bear some similarity with the case of the one-dimensional SOC of linear momentum. However unlike the momentum, here the orbital angular momentum $m$ is quantized, which essentially alters the many-body ground state when the atom-atom interaction is included.

In angular momentum space, the interaction Hamiltonian takes the form of $H_{\text{int}}^{\text{ring}} = g\sum_{mm'k} \mathbf{\Psi}^\dagger_{m+k\uparrow}\mathbf{\Psi}^\dagger_{m'-k\downarrow}\mathbf{\Psi}_{m'\downarrow}\mathbf{\Psi}_{m\uparrow}$, which conserves the total angular momentum. It is natural to introduce a general pairing field $\Delta_Q = g\sum_m \langle \mathbf{\Psi}_{Q-m\downarrow}\mathbf{\Psi}_{m\uparrow}\rangle$ describing the pairing between atoms with angular momenta $m$ and $Q - m$, and write the mean-field Hamiltonian as

$$H_{\text{MF}} = \frac{1}{2}\sum_m \mathbf{\Phi}^\dagger_{m,Q}\begin{pmatrix} H_{\text{ring}}(m) & \Delta_Q \\ \Delta_Q & -\sigma_y H^*_{\text{ring}}(Q-m)\sigma_y \end{pmatrix}\mathbf{\Phi}_{m,Q} + \sum_m \xi_{Q-m} - \frac{|\Delta_Q|^2}{g}, \tag{4}$$

where $\mathbf{\Phi}_{m,Q} = [\mathbf{\Psi}_{m\uparrow}, \mathbf{\Psi}_{m\downarrow}, \mathbf{\Psi}^\dagger_{Q-m\downarrow}, -\mathbf{\Psi}^\dagger_{Q-m\uparrow}]^T$ and $\xi_m = m^2/2R^2 - \mu$. Noticing that in the angular space, the above introduced finite orbital angular momentum pairing exactly gives the phase configuration of a vortex state with vorticity $Q$, i.e., $\Delta = \Delta_Q e^{iQ\phi}$.

In general, the ground state can be obtained by first minimizing the energy $E_Q^{\text{MF}} \equiv \langle H_{\text{MF}}\rangle = \sum_m \xi_{|Q-m|} + \sum_{m,\nu}\Theta(-E_{m,\nu})E_{m,\nu} - |\Delta_Q|^2/g$ for each $Q$, and then further minimizing on $Q$. Here for illustration, we plot the phase boundaries [see the dashed lines in Fig. 2(a)] by comparing the free energies of different phases with the parameters used in the numerics. The agreement between the numerical simulations and the mean-field results validates the approximation adopted above, and suggests that the single vortex states originating from the finite orbital angular momentum pairing.

Physically, as the Raman coupling and two-photon detuning serve as effective transverse and longitudinal Zeeman fields, the interplay with the SOAMC leads to the asymmetric dressed Fermi surface in the angular momentum space. The pairing with opposite angular momentum is no longer energetically favorable; instead the pairing happens between fermions with angular momentum $l_1$ and $-l_2$ ($l_1 \neq l_2$). As a result, the total angular momentum carried by the pairing order parameter is $Q = l_1 + (-l_2) \neq 0$, yielding the vortex-$Q$ states in the ground-state phase diagram, where $Q$ is quantized and increases discontinuously with the two-photon detuning. Furthermore, when the Fermi surface (or the chemical potential) is on the upper branches, pairing may take place

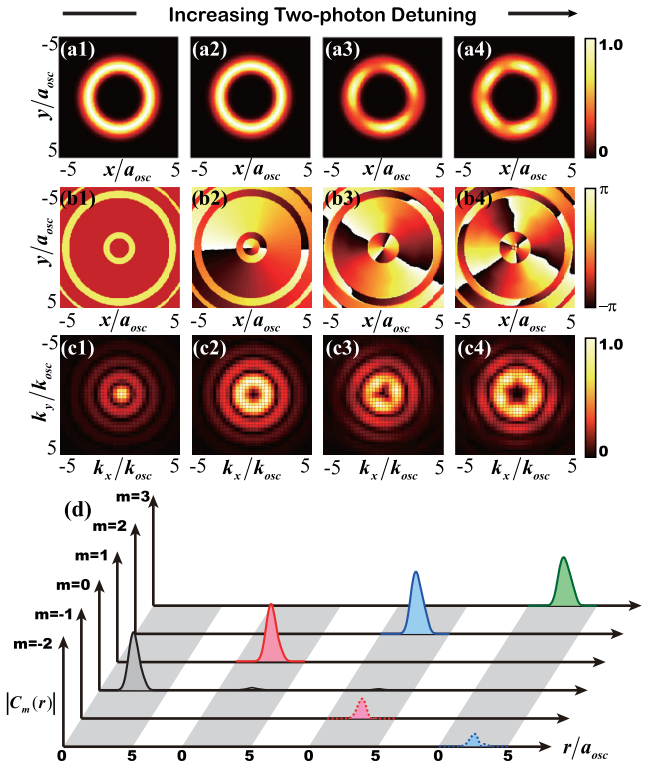


FIG. 3. The amplitude (a1)–(a4) and phase (b1)–(b4) distributions of the order parameter $\Delta(r)$ in the $x$-$y$ plane for different two-photon detuning $\delta/E_F = 0$, 0.1, 0.3, and 0.4. (c1)–(c4) The corresponding momentum distributions $|\Delta(k_x, k_y)|$. (d) The radial distributions $|C_m(r)|$ of the $m$ component for order parameters in (a1)–(a4), respectively. Other parameters are $\chi/E_F = 0.7$, $E_b/E_F = 0.3$, $\Omega/E_F = 0.14$, and the unit of momentum $k_{\rm osc} = \sqrt{2\omega_r}$.

in multichannels with different angular momenta, which may give rise to exotic vortex states with peculiar features.

*Exotic vortex with discrete rotational symmetry.*—In Fig. 3, we show the evolution of the ground state as a function of two-photon detuning $\delta$ for a relatively weak two-photon Rabi frequency $\Omega/E_F = 0.14$. One can see that with the increasing of $\delta$, the NS state with $Q = 0$ [Figs. 3(a1),3(b1),3(c1)] first transits into a single vortex state with $Q = 1$ [Figs. 3(a2)–3(c2)], both preserving the continuous rotational symmetry. The momentum distribution of a NS state is always peaked at zero momentum [Fig. 3(c1)], in sharp contrast to the vortex states with a nearly vanishing contribution from zero momentum but peaks at finite $k_r$ [Figs. 3(c2)–3(c4)]. When further increasing $\delta$, two exotic vortex states become the ground state sequentially [Figs. 3(a3),3(a4)]. Different from the vortex state governed by a single orbital-angular-momentum pairing, we find the exotic vortex state has two different pairing components with angular momentum $Q_1$ and $Q_2$ [referred to as Fig. 3(d)], by which we can write $\Delta(r, \phi) \sim \sum_{m=Q_1,Q_2} C_m(r) e^{im\phi}$ with $C_m(r)$ the amplitude of $m$ component. Consequently, a spontaneous periodical modulation on the spatial profile of the order parameter $|\Delta|^2 \sim C_{Q_1}^2 + C_{Q_2}^2 + 2C_{Q_1}C_{Q_2}\cos(Q_1 - Q_2)\phi$ is developed along the azimuthal direction, which breaks the continuous rotational symmetry into a discrete $M$-fold rotational symmetry with $M = |Q_1 - Q_2|$ in both real and momentum spaces. Note that the two components are, in general, unequally weighted, and the winding number of the exotic vortex is determined by the stronger one. To our knowledge, the emergence of this type of spontaneous-symmetry-breaking vortex states, as a consequence of an intricate interplay between atom-atom interaction, two-photon detuning, and SOAMC in a nevertheless experimentally accessible setup, bears no precedent examples in the literature.

Now we address the effect of quantum fluctuation, which has been neglected so far but is inevitable in experiments. In general, the pairing fluctuation may deplete the mean-field ground states and lead to the "Lee-Huang-Yang" corrections on the ground-state energy [45,46]. Such corrections can be taken into account by writing the pairing field as $\Xi = \Delta + \varphi$, with $\varphi$ the pair fluctuation around the mean-field $\Delta$, and then evaluating the noncondensed pair density $n_b = \langle \varphi^\dagger \varphi \rangle$ in the modified total atom number $N_{\rm atom} = \int d\mathbf{r}[\sum_\sigma n_\sigma(\mathbf{r}) + 2n_b(\mathbf{r})]$ (see the Supplemental Material [42] for details). By self-consistently solving the BdG equations with the modified number equation, we find that in all cases under our consideration the quantum depletion due to the pairing fluctuation is insignificant ($\lesssim 8\%$ of the total atoms) [42]. The resultant corrections on the order parameter, which can be characterized by the deviation ratio $\mathcal{D}(\Delta, \tilde{\Delta}) = \sqrt{\int |\tilde{\Delta}(\mathbf{r}) - \Delta(\mathbf{r})|^2 d\mathbf{r}} / \sqrt{\int |\Delta(\mathbf{r})|^2 d\mathbf{r}}$ between the corrected pairing order parameter $\tilde{\Delta}$ and the mean field $\Delta$, are also weak with $\mathcal{D}(\Delta, \tilde{\Delta}) \lesssim 6\%$ and the weights contributed by different angular momentum components nearly unchanged (see the Supplemental Material for details [42]). Thus we conclude that the ground state configurations originally obtained from mean field calculations are generally robust against the corrections due to quantum fluctuation.

*Experimental detection.*—We first discuss the possible energy scales in experiment. For example, one can choose $E_F \sim 2\pi \times 3.1$ kHz of a 2D Fermi gas [47], the Raman coupling strength $\Omega \sim 2\pi \times (0.5$–$1)$ kHz, the two-photon detuning $\delta \sim 2\pi \times (0$–$2)$ [33–35] and $\chi \sim 2\pi \times 2.2$ kHz [48], and tune $E_B$ via Feshbach resonance [49] to address the whole regime of the phase diagram in this work. In experiment, the vortex states can be characterized by the total angular momentum $Q$ by measuring the collective shift of the radial quadrupole modes [50–52]. Further, to reveal the exotic vortex phases with discrete rotational symmetry, we turn to their atomic density distributions $n(\mathbf{r})$, which can be directly measured by *in situ* absorption imaging [53,54]. In Fig. 4, we plot $n(\mathbf{r}) = \sum_\sigma n_\sigma(\mathbf{r})$ for the typical vortex phases discussed above. The reduction from

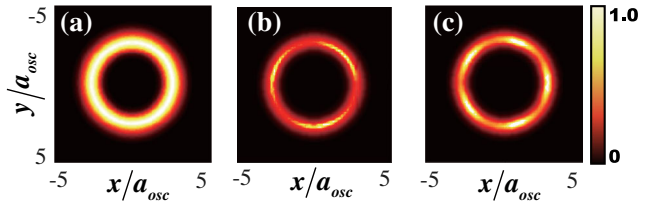


FIG. 4. The normalized density distributions of $n(\mathbf{r})$ for different vortex states in Fig. 3: (a) a single vortex state with rotational symmetry for $\delta/E_F = 0.1$, (b) an exotic vortex with $\mathcal{C}_3$ symmetry for $\delta/E_F = 0.3$, and (c) an exotic vortex with $\mathcal{C}_5$ symmetry for $\delta/E_F = 0.4$.

a continuous rotational symmetry to a discrete one can be clearly identified in the density profile, for example, a $\mathcal{C}_3$ ($\mathcal{C}_5$) symmetry in Figs. 4(b),4(c). This distinguishes the exotic vortex states from the single vortex with rotational symmetry.

*Conclusion.*—In summary, we have studied the superfluid ground state of a two-dimensional Fermi gas with SOAMC. Because of the finite orbital angular momentum pairing induced by the SOAMC and two-photon detuning, a family of vortex states with unique features are predicted to be the ground state in a broad regime of the phase diagram. Specifically, an exotic vortex which breaks the rotational symmetry spontaneously may appear. These results reveal the nontrivial physics brought by SOAMC, and open an avenue to search unusual quantum vortex and superfluid phases.

We would like to thank G. Juzeliūnas, Yong Sun, Wenjun Shao, and Changan Li for interesting discussions. This work was supported by NSFC under Grants No. 11875195, No. 11474205, foundation of Beijing Education Committees under Grants No. CITTCD201804074, and No. KZ201810028043, and foundation of Zhejiang Province Natural Science under Grant No. LQ20A040002. J. L. acknowledges support from National Natural Science Foundation of China under Project 11774317. Q. S. and A.-C. J acknowledge support from the key research project of Academy for Multidisciplinary Studies, Capital Normal University. The numerical calculations in this paper have been done on the supercomputing system in the Information Technology Center of Westlake University.

*Note added in the proof.*—We came to notice a related work [55], where a giant vortex is discussed in a different configuration.

*sunqing@cnu.edu.cn
†lijian@westlake.edu.cn

[1] Y.-J. Lin, K. Jiménez-García, and I. B. Spielman, Nature (London) **471**, 83 (2011).
[2] P. J. Wang, Z.-Q. Yu, Z. K. Fu, J. Miao, L. H. Huang, S. J. Chai, H. Zhai, and J. Zhang, Phys. Rev. Lett. **109**, 095301 (2012).
[3] L. W. Cheuk, A. T. Sommer, Z. Hadzibabic, T. Yefsah, W. S. Bakr, and M. W. Zwierlein, Phys. Rev. Lett. **109**, 095302 (2012).
[4] V. Galitski and I. B. Spielman, Nature (London) **494**, 49 (2013).
[5] L. Huang, Z. Meng, P. Wang, P. Peng, S.-L. Zhang, L. Chen, D. Li, Q. Zhou, and J. Zhang, Nat. Phys. **12**, 540 (2016).
[6] Z. Wu, L. Zhang, W. Sun, X.-T. Xu, B.-Z. Wang, S.-C. Ji, Y. Deng, S. Chen, X.-J. Liu, and J.-W. Pan, Science **354**, 83 (2016).
[7] H. Hu, L. Jiang, X. J. Liu, and H. Pu, Phys. Rev. Lett. **107**, 195304 (2011).
[8] C. Chen, Phys. Rev. Lett. **111**, 235302 (2013).
[9] F. Wu, G. C. Guo, W. Zhang, and W. Yi, Phys. Rev. Lett. **110**, 110401 (2013).
[10] C. Qu, Z. Zheng, M. Gong, Y. Xu, L. Mao, X. Zou, G. Guo, and C. Zhang, Nat. Commun. **4**, 2710 (2013).
[11] W. Zhang and W. Yi, Nat. Commun. **4**, 2711 (2013).
[12] J. P. A. Devreese, J. Tempere, and C. A. R. Sá de Melo, Phys. Rev. Lett. **113**, 165304 (2014).
[13] Z. Zheng, C. Qu, X. Zou, and C. Zhang, Phys. Rev. Lett. **116**, 120403 (2016).
[14] L.-L. Wang, Q. Sun, W.-M. Liu, G. Juzeliūnas, and A.-C. Ji, Phys. Rev. A **95**, 053628 (2017).
[15] Q. Sun, L.-L. Wang, X.-J. Liu, G. Juzeliūnas, and A.-C. Ji, Phys. Rev. A **99**, 043601 (2019).
[16] J. Leonard, A. Morales, P. Zupancic, T. Esslinger, and T. Donner, Nature (London) **543**, 87 (2017).
[17] J.-R. Li, J. Lee, W. Huang, S. Burchesky, B. Shteynas, F. C. Top, A. O. Jamison, and W. Ketterle, Nature (London) **543**, 91 (2017).
[18] R. Bombin, J. Boronat, and F. Mazzanti, Phys. Rev. Lett. **119**, 250402 (2017).
[19] W. S. Cole, S. Zhang, A. Paramekanti, and N. Trivedi, Phys. Rev. Lett. **109**, 085302 (2012).
[20] J. Radić, A. DiCiolo, K. Sun, and V. Galitski, Phys. Rev. Lett. **109**, 085303 (2012).
[21] Z. Cai, X. Zhou, and C. Wu, Phys. Rev. A **85**, 061605(R) (2012).
[22] X. Zhang, W. Wu, G. Li, W. Lin, Q. Sun, and A.-C. Ji, New J. Phys. **17**, 073036 (2015).
[23] J.-Y. Zhang, S.-C. Ji, Z. Chen, L. Zhang, Z.-D. Du, B. Yan, G.-S. Pan, B. Zhao, Y.-J. Deng, H. Zhai, S. Chen, and J.-W. Pan, Phys. Rev. Lett. **109**, 115301 (2012).
[24] L. W. Cheuk, A. T. Sommer, Z. Hadzibabic, T. Yefsah, W. S. Bakr, and M. W. Zwierlein, Phys. Rev. Lett. **109**, 095302 (2012).
[25] C. Qu, C. Hamner, M. Gong, C. Zhang, and P. Engels, Phys. Rev. A **88**, 021604(R) (2013).
[26] C. Hamner, C. Qu, Y. Zhang, J. Chang, M. Gong, C. Zhang, and P. Engels, Nat. Commun. **5**, 4023 (2014).
[27] S. Ji, J. Zhang, L. Zhang, Z. Du, W. Zheng, Y. Deng, H. Zhai, S. Chen, and J.-W. Pan, Nat. Phys. **10**, 314 (2014).
[28] Z. Meng, L. Huang, P. Peng, D. Li, L. Chen, Y. Xu, C. Zhang, P. Wang, and J. Zhang, Phys. Rev. Lett. **117**, 235304 (2016).

[29] J. Li, W. Huang, B. Shteynas, S. Burchesky, F. C. Top, E. Su, J. Lee, A. O. Jamison, and W. Ketterle, Phys. Rev. Lett. **117**, 185301 (2016).
[30] K. Sun, C. Qu, and C. Zhang, Phys. Rev. A **91**, 063627 (2015).
[31] C. Qu, K. Sun, and C. Zhang, Phys. Rev. A **91**, 053630 (2015).
[32] M. DeMarco and H. Pu, Phys. Rev. A **91**, 033630 (2015).
[33] H.-R. Chen, K.-Y. Lin, P.-K. Chen, N.-C. Chiu, J.-B. Wang, C.-A. Chen, P.-P. Huang, S.-K. Yip, Y. Kawaguchi, and Y.-J. Lin, Phys. Rev. Lett. **121**, 113204 (2018).
[34] P.-K. Chen, L.-R. Liu, M.-J. Tsai, N.-C. Chiu, Y. Kawaguchi, S.-K. Yip, M.-S. Chang, and Y.-J. Lin, Phys. Rev. Lett. **121**, 250401 (2018).
[35] D. Zhang, T. Gao, P. Zou, L. Kong, R. Li, X. Shen, X.-L. Chen, S.-G. Peng, M. Zhan, H. Pu, and K. Jiang, Phys. Rev. Lett. **122**, 110402 (2019).
[36] L. Allen, M. W. Beijersbergen, R. J. C. Spreeuw, and J. P. Woerdman, Phys. Rev. A **45**, 8185 (1992).
[37] M. Babiker, W. L. Power, and L. Allen, Phys. Rev. Lett. **73**, 1239 (1994).
[38] H. He, M. E. J. Friese, N. R. Heckenberg, and H. Rubinsztein-Dunlop, Phys. Rev. Lett. **75**, 826 (1995).
[39] L. Marrucci, E. Karimi, S. Slussarenko, B. Piccirillo, E. Santamato, E. Nagali, and F. Sciarrino, J. Opt. **13**, 064001 (2011).
[40] Y. Duan, Y. M. Bidasyuk, and A. Surzhykov, Phys. Rev. A **102**, 063328 (2020).
[41] X.-L. Chen, S.-G. Peng, P. Zou, X.-J. Liu, and Hui Hu, Phys. Rev. Research **2**, 033152 (2020).
[42] See the Supplemental Material at http://link.aps.org/supplemental/10.1103/PhysRevLett.126.193401 for the derivation of the model and single-particle energy spectrum, and the self-consistent calculation of the real-space Bogoliubov–de Gennes equation and the Gaussian pairing fluctuations in the numerical simulations, which includes Ref. [43].
[43] H. Kleinert, Fortsch. Phys. **26**, 565 (1978).
[44] M. Randeria, J.-M. Duan, and L.-Y. Shieh, Phys. Rev. Lett. **62**, 981 (1989).
[45] T. D. Lee, K. Huang, and C. N. Yang, Phys. Rev. **106**, 1135 (1957).
[46] V. M. Galitskii, Zh. Eksp. Teor. Fis. **34**, 151 (1958) [Sov. Phys. JETP **7**, 104 (1958)].
[47] K. Hueck, N. Luick, L. Sobirey, J. Siegl, T. Lompe, and H. Moritz, Phys. Rev. Lett. **120**, 060402 (2018).
[48] K. C. Wright, L. S. Leslie, and N. P. Bigelow, Phys. Rev. A **78**, 053412 (2008); K. C. Wright, L. S. Leslie, A. Hansen, and N. P. Bigelow, Phys. Rev. Lett. **102**, 030405 (2009).
[49] C. Chin, R. Grimm, P. Julienne, and E. Tiesinga, Rev. Mod. Phys. **82**, 1225 (2010).
[50] F. Chevy, K. W. Madison, and J. Dalibard, Phys. Rev. Lett. **85**, 2223 (2000).
[51] E. Hodby, S. A. Hopkins, G. Hechenblaikner, N. L. Smith, and C. J. Foot, Phys. Rev. Lett. **91**, 090403 (2003).
[52] S. Riedl, E. R. S. Guajardo, C. Kohstall, J. H. Denschlag, and R. Grimm, New J. Phys. **13**, 035003 (2011).
[53] C. C. Bradley, C. A. Sackett, and R. G. Hulet, Phys. Rev. Lett. **78**, 985 (1997).
[54] M. C. Revelle, J. A. Fry, B. A. Olsen, and R. G. Hulet, Phys. Rev. Lett. **117**, 235301 (2016).
[55] K.-J. Chen, F. Wu, S.-G. Peng, W. Yi, and L. He, Phys. Rev. Lett. **125**, 260407 (2020).